GLAST: the Gamma–Ray Large Area Space Telescope

John F. Krizmanic [1]
for the GLAST Collaboration [1]

USRA/NASA Goddard Space Flight Center, Greenbelt, MD 20771 USA

Abstract

Initiated by the spectacular successes of the Energetic Gamma Ray Experiment Telescope (EGRET) aboard the Compton Gamma Ray Observatory, the Gamma ray Large Area Space Telescope (GLAST) collaboration has been developing a next generation, high energy gamma ray experiment. The goal of the GLAST mission is to image photons with sufficient angular resolution for unique, point source identification in the energy range of 10 MeV to greater than 100 GeV with good energy resolution and with a large field of view. Operating as a pair-conversion telescope, GLAST will use silicon microstrip detectors interspersed with thin layers of high-Z material to form an upper, tracker section which will be followed by a 10 radiation length deep, segmented calorimeter. The large area required to achieve the desired sensitivity and the development of ultralow-power electronics has led to a baseline configuration employing over 87 m^2 of silicon microstrip detectors with approximately 1.3×10^6 channels. The GLAST instrument will operate with the tracker and the calorimeter acquiring data asynchronously and semi-independently, thus self-triggering on events as they occur.

Key words: Silicon detectors; space.

1 Introduction

Gamma ray astronomy offers a unique window to the high energy processes in the universe [2]. Gamma rays are relatively unattenuated and unscattered at the source while their trajectories are unaffected by magnetic fields and, therefore, point directly back to their source. Furthermore, the mean free path of gamma rays in the universe is large (up to redshifts of $Z \approx 5$) [3], thus

[1] jfk@cosmicra.gsfc.nasa.gov

gamma rays contain information on the cosmological scale. When considered with measurements at other wavelengths, gamma ray measurements provide invaluable information needed to understand the astrophysics at the source.

Gamma ray telescopes must be located in Earth orbit or beyond as gamma rays are strongly attenuated in the atmosphere. Extraterrestrial gamma rays are relatively rare; the flux at 1 GeV from the brightest, continuously emitting region of the sky, the galactic center, is approximately 10^{-4} photons/(cm^2 $\cdot$ sr $\cdot$ s $\cdot$ GeV) falls as E^{-2} [4]. Thus the backgrounds due to cosmic ray and gamma ray induced, atmospheric secondaries are prohibitively large for any suborbital experiment. The first definitive detection of high energy (mainly) galactic gamma rays was by the OSO-3 mission in 1968. This has been followed by a string of extremely successful high energy gamma ray imaging telescopes starting with the SAS-2 mission (1972) which was followed by the COS-B mission (1975) which also incorporated a calorimeter in the instrument.

With the launch of the Compton Gamma Ray Observatory in 1991, the EGRET instrument has revolutionized the field of high energy, gamma ray astronomy with its unparalleled measurements in the extended energy range of 30 MeV $\rightarrow$ 30 GeV [2]. An all-sky measurement is shown in Figure 1. EGRET consists of a tracking chamber employed as a pair-conversion telescope followed by a 7.8 X_0 deep, monolithic calorimeter. Phenomena such as gamma ray emission associated with solar flares, galactic and extragalactic diffuse gamma ray emission, gamma radiation from pulsars, gamma ray bursts, and active galactic nuclei (AGN's) have been studied by EGRET and have led to a deeper understanding of some of the highest energy processes in the observed universe.

Given the success of the EGRET mission, which is anticipated to end in the next few years, there is a strong interest in developing a next generation, high energy gamma ray telescope. The wealth of EGRET measurements has led to a deeper understanding of the universe, yet has also raised many questions. Figure 2 illustrates the observed point sources of photons with energy greater than 100 MeV from the Second EGRET Catalog [5]. As the figure illustrates, approximately half of the sources are not identified with any previously observed astrophysical objects. A new instrument with appropriate improvements in angular resolution and sensitivity would vastly improve the ability to to recognize these unidentified sources.

Using EGRET as a metric, this new instrument should have

(1) A larger active area and higher efficiency for increased source sensitivity,
(2) Improved angular resolution of reconstructed photons for accurate source identification,
(3) An energy range extended to several hundred GeV with the goal of over-

lapping that for ground based γ telescopes [6],
(4) A larger field of view,
(5) A robust design and long lifetime.

In addition, the instrument must be able to move from an all-sky monitoring mode to a pointed survey mode once an event of interest is detected by either GLAST or other experiments.

The EGRET measurements have helped solidify a unified picture of AGN's. A massive black hole at the center is being fed by an accretion disk which is in turn surrounded by a thick torus of cooler gas. Sometimes, jets of particles emerge from the disk. Thus, different classes of AGN's appear differently as they are viewing at different angles, e.g. one is looking down the jet in blazars. Figure 3 shows the power spectrum as a function of photon frequency for an AGN [7]. As is clearly evident, the spectrum is dominated by the gamma ray contribution. The high energy, gamma ray luminosity from AGN's is rapidly variable and can reach as high as 10^{46} ergs/sec including beaming effects [2]. A new instrument with higher sensitivity could determine if the observed, extragalactic diffuse gamma ray background is caused by unresolved AGN's. AGN's have also been observed in the TeV range by ground based arrays, and comparisons with EGRET measurements imply that a spectral change exists at an energy greater than 30 GeV on some sources [6]. A new instrument with an extended energy range would provide this measurement. AGN's have been observed with high redshifts ($Z \approx 4$). Assuming AGN spectra are well understood, these objects could be used as a probe of extragalactic background light (EBL) during galaxy formation in the early universe via $\gamma\gamma_{EBL} \rightarrow e^+e^-$ attenuation [8].

The ability to measure photons with energy greater than 30 GeV opens up an entire new region of astrophysical investigation. As well as measuring a spectral cut off for AGN's, an extended energy range leads to a sensitivity to WIMP annihilation [9]. WIMP's, such as the lightest supersymmetric particle, are candidates for dark matter, and an annihilation line or bump in the diffuse gamma ray background would provide a signature. As the WIMP's would be confined to the galactic halo, an observation of an asymmetry as a function of the viewed line of site would provide further evidence.

A high energy, gamma ray instrument with increased sensitivity and angular resolution would yield measurements on other astrophysical phenomena. These include accurately determining the extragalactic component of the high energy gamma ray flux and definitively observing the acceleration of cosmic rays by supernovae remnants. Observations of additional gamma ray pulsars such as Geminga would help in the understanding of the pulsar mechanisms, especially at high energy. Furthermore, the increased sensitivity could lead to the observation of a copious number of high energy gamma ray bursts [10].

2 The GLAST Instrument

The GLAST collaboration has been developing such a next generation, high energy gamma ray experiment, and a conceptual picture of the instrument is shown in Figure 4. The instrument is comprised of an upper tracker section which uses silicon microstrip detectors in a pair-conversion telescope, followed by a 10 X_0 deep segmented calorimeter. A mosaic of segmented scintillator counters, not shown in the figure, surround the tracker and form a veto shield to reject the acceptance of cosmic ray induced triggers in the instrument. The instrument will acquire data asynchronously, and the onboard system software will perform at a high level the event reconstruction and background rejection.

The tracker section is sub-divided into a modular structure, yielding a robust design which minimizes any potential effects against common-mode failures. Each module, denoted as a tower, is comprised of a mechanical structure and individual trays. Each tray is comprised of a thin plate of high-Z radiator, a mechanical support structure, and two planes of single-sided, AC-coupled silicon microstrip detectors. Each plane of microstrip detectors is arranged such that the strips of one plane are orthogonal to the other, yielding an x, y position measurement of the traversing charged particles. This current baseline for the tracker will employ over 87 m^2 of silicon microstrip detectors with approximately 1.3×10^6 readout channels interleaved with a total of 0.5 X_0 of radiators.

The baseline calorimeter design uses 3 cm $\times$ 3 cm $\times$ 10 X_0 CsI logs which share the modular configuration of the upper tracker. The calorimeter research and development effort is investigating the use of other CsI geometries in several configurations and, in a disparate effort, the use of scintillating fiber/absorber sheet ('spaghetti') calorimetry. Thus as the design evolves, the calorimeter may or may not share the same modular structure as the tracker. The calorimeter is to collect data semi-autonomously and will measure the approximately 60% of the gamma rays which do not interact in the tracking section. Thus, the segmentation of the calorimetry will provide for source imaging albeit not with the resolution of the tracker [11].

The performance goals of the GLAST instrument are summarized in Table 1. In order to model GLAST in detail, a Monte Carlo program, GIZMO, has been developed [12]. The GLAST instrument has also been modeled using the GEANT package which provides an alternate simulation methodology [13,14]. Some of the results from Monte Carlo studies of the initial instrumental baseline are shown in Figure 5 as a function of incident photon energy and angle. The results for the EGRET instrument are also shown for comparison. Thus, GLAST will have approximately 30 times the sensitivity as compared to that for EGRET at comparable energies [3].

The majority of the luminosity of most astrophysical sources is at lower energies as they have an exponentially decreasing spectrum. However, GLAST will open up a new energy scale of investigation at photon energies greater than 30 GeV. Thus, the instrumental design is driven by these dissimilar requirements. At the lower energies, the effective area of the instrument decreases due to the nature of the pair production process. Furthermore, the effects of multiple scattering worsen the angular resolution of the instrument at these lower energies.

The lower energy angular resolution improves as the number of measured tracking points are increased while appropriately decreasing the thickness of the radiators while keeping the total X_0 constant. Increasing the sensitivity would involve increasing the area of the instrument or the number of converter and tracking planes. However, the practical aspect of a power budget fixes the maximum number of readout channels. This in turn determines the maximum number of tracking layers for a given instrumental area. At higher energies, the sensitivity of the instrument will be mainly determined by the calorimetry while the angular resolution is set by the positional resolution of the tracking detector. Thus, the extremes of the instrumental energy range lead to competing requirements for the allocation of readout channel density and must be balanced in the final design.

The GLAST instrument must reject the background induced in the instrument by the interactions of cosmic ray nuclei with a rejection factor of at least 10^4. This is to be accomplished by the use of a multi-level trigger architecture enabled in both hardware and software. The goal is to create a flexible triggering environment with a high reliance on onboard software. Thus, the triggering algorithms will have the capability to become more efficient as the experiment evolves. The onboard software will allow for calibration modes, such as using charged cosmic rays as an inflight diagnostic. The system must also provide the necessary monitoring and control while being highly fault tolerant. Initial estimates employing a three-level triggering architecture have demonstrated a sufficient reduction of cosmic ray and albedo gamma ray backgrounds, while efficiently identifying extraterrestrial gamma rays without requiring an unreasonably high data downlink capability [15].

2.1 The GLAST Tracker

Silicon microstrip detectors offer many advantages over other tracking technologies for space-based applications. These include high efficiency, extremely low dead time, and fast response, excellent multi-hit and positional resolution, no 'consummables', modest operational voltages, and a long lifetime even in a radiation environment. Silicon microstrip detectors provide a robust technol-

ogy and have been proven to work reliably in large channel count systems such as the LEP and CDF collider experiments. Recent advances in ultralow-power, asynchronous readout electronics have allowed this silicon microstrip technology to be seriously considered for space-based instruments with greater than 10^6 readout channels while using only a few hundred watts. Thus, satisfying the severe power constraints of a space-based mission with an extremely large channel count is conceivable.

The current baseline for the tracker employs 5×5 towers with each tower comprised of seventeen mechanical trays. This arrangement yields sixteen pairs of x, y measurements while 0.0385 X_0 radiators are located on the bottom thirteen trays. The tower walls are comprised of 3 mm of beryllium and serve as both the mechanical support for the trays and as a thermal conduit to remove the heat of the electronics. Tests using a Delta-II vibrational profile have demonstrated the mechanical stability of the tray design [16]. Initial thermal modeling has indicated that this design will provide sufficient thermal paths and gradients to allow for detector operation in a temperature range of $5^\circ \rightarrow 25^\circ$ C [17].

Figure 6 illustrates the tray design and their incorporation into a tower. The current baseline uses five ladders, comprised of five 6.4×6.4 cm^2 $\times$ 385 μm detectors wire bonded together to form each detector plane. The ladders are to be attached to a low-grammage, low-Z mechanical structure formed by either a composite and honeycomb or a foam structure with the readout electronics interfaced on the sides. In order to minimize the effects of multiple scattering, the radiators are located as near a silicon microstrip detector plane as possible and the separation between the individual x and y measuring planes is minimized.

The angular resolution of GLAST has been modeled in detail using GIZMO, and the results are shown in Figure 7 which details the improvement over the initial instrument baseline for a variety of configurations [18]. This has led to the current baseline of sixteen pairs of x, y planes in each module of the tracker with 0.0385 X_0 radiators. The detector size and 195 μm pitch lead to 320 channels per detector, 5.12×10^4 channels per module, and a total of approximately 1.28×10^6 for the entire tracker.

The current GLAST tracker baseline uses single-sided instead of double-sided silicon microstrip detectors. The motivation is that double-sided detectors tremendously increase the complexity of the detector design, fabrication, and the instrument itself. Furthermore, the orthogonal interconnects required on each side are highly non-trivial. A portion of the possible gain is illustrated in Figure 7 by the points labeled DSSD. The improvement in performance is most pronounced at the lower energies where the effects of multiple scattering dominate. However, the improvement in angular resolution is at the 20% level.

Based on this result alone, it is difficult to justify the increased cost and complexity.

However, another possible scientific gain is offered by the ability to measure the polarization of the photon. Polarization measurements would provide another mechanism for understanding the astrophysics at the source. Experimentally, the ability to measure the polarization using the azimuthal angles of the created electron-positron pair is suppressed exponetially by the effects of multiple scattering and track reconstruction errors. Thus, these effects must be minimized. Monte Carlo studies have indicated that with the use of sufficiently thin double-sided microstrip detectors and radiators, GLAST would have the capability to determine the polarization of photons emitted from highly polarized, bright sources on a modest observational timescale [19]. The use of two similar thickness, single-sided detectors to perform the tracking measurements degrades the polarization signal, albeit polarization measurements still may be possible with much longer source observation times.

2.2 GLAST Silicon Microstrip Detector Development

Hamamatsu Photonics has fabricated GLAST prototype detectors, and their operational properties have been characterized [20]. The single-sided detectors were fabricated on four inch, 500 μm thick wafers with a strip implant length of 5.8 cm and width of 57 μm. The detectors are AC-coupled, 'punch through' biased, and have 236 μm strip pitch. Characterization testing has yielded leakage currents per strip of approximately 700 pAmps to 1.8 nAmps at full depletion, while the depletion voltage varies from approximately 110 to 150 volts. The total capacitance of a strip has been measured to be yielding an interstrip capacitance of 0.62 pF/cm and a body capacitance of 0.55 pF/cm (1.17 pF/cm total). This agrees fairly well with the strip capacitance anticipated using a numerical calculation [20]. Additionally, measurements of the effects of irradiation and charge collection studies have been performed [21]. Using gamma rays from ^{60}Co, a 10 kRad exposure leads to an increase in the leakage current of approximately 2.8 nAmp/cm. The charge collection studies indicated that for a sufficiently long electronic shaping time, i.e. $\tau > 1$ μsec, the larger strip pitch does not induce an inefficiency.

A new detector order is being fabricated by Hamamatsu Photonics and possibly Seiko with an initial delivery at the end of 1997. The 6.4 cm $\times$ 6.4 cm $\times$ 385 μm detectors are single-sided, AC coupled, biased with 50 MΩ poly-silicon resistors, and will have 195 μm strip pitch. The 50 μm wide metallization over the coupling capacitor oxide will be patterned such that two separate metal lines joined by bridges will run over the implanted strip. If a defect in the oxide exists under one of the strips, the bridges can be cut

forming a narrower, yet operating, strip. Thus, the effective yield of detector fabrication will be increased. Using the capacitance modeling routines used with the prototype measurements, the capacitance of 195 μm pitch, 385 μ thick detectors is predicted to be 1.12 pF/cm which yields a total capacitance of approximately 35 pF for a five detector long ladder assuming 6.2 cm long strips on each detector [22].

The research and development effort of the silicon microstrip detectors has begun to address detector optimization issues. Inherent in any design which uses microstrip detectors is the existence of dead areas on the periphery of the detectors. The problem is two-fold: A traversing particle's position is not measured, and the dead space between detectors provides an additional scattering medium. This problem is further exacerbated when detectors are arranged in a tiled structure such as ladders. Nominal design rules call for a dead length outside the active area of a microstrip detector of twice the thickness of the detector. As GLAST will use approximately 400 μm thick detectors, this leads a substantial dead area especially in a five-detector-long ladder. Two solutions to this problem are under investigation. The first involves minimizing the dead area outside the active portion of a detector without adversely affecting its operational properties. The second pertains to the detector size itself. Detectors fabricated on six inch wafers could be 8×8 cm^2, and a 32 cm ladder could be formed by four of these detectors versus five of the 6.4×6.4 cm^2 detectors. The number of ladders would also be reduced from five to four.

2.3 GLAST Electronics Development

Given the low total power ($\approx$ 300 watts) available for the GLAST tracker, the front-end electronics (FEE) must amplify, sparsify, and multiplex the signals induced on the silicon microstrip detectors using no more that 200 μwatts/channel while employing a few μsec shaping time. The FEE ASIC's are to operate asynchronously, be radiation hard to at least 10 kRad, and have a redundant design to avoid catastrophic common-mode failures. Sufficient event buffering must exist to minimize the deadtime while the RMS noise and noise occupancy must be minimized.

The performance and power requirements required by the GLAST mission have led to the development of ultralow-power ASIC electronics [23]. Based on the HP 0.8 μm process, a 16 channel prototype ASIC has been fabricated and tested. The ASIC uses FETs in a cascode arrangement for the charge pre-amplifier followed by a shaping amplifier. The gain of the ASIC has been measured to be 150 mV/fC for a shaping time of 1.6 μsec. The resultant signals are discriminated to yield a digital output which is then multiplexed. The ASIC demonstrated a noise performance of $N_{ENC} = 204 + 30\ C_{Strip}$ (pF) e$^-$

using only 150 μW/channel. Table 2 lists the testing results for a variety of configurations. The channel-to-channel variations in the threshold determination were measured to be 430 e^- (RMS), which is adequate considering the signal of 32,000 e^--hole/pairs created in a 400 μm thick detector.

A 32 channel prototype ASIC using the same process and sharing the same front-end components has been fabricated. New features include sparse readout with an ordered, formatted list of triggered channels, multiple event buffering, and differential, low-voltage signal transmission. A unique feature of this FEE ASIC is that it is clocked only when necessary to minimize the power required for operation. Initialization, calibration, and readout is handled by a control chip on each side of a chain of FEE ASIC's, and a sketch of the architecture is shown in Figure 8. Any FEE ASIC can be controlled and pass data from left to right or vice versa, thus minimizing the possible impact of FEE ASIC failures. Presently, a 64 channel full scale prototype of the FEE ASIC's is in the design phase.

The asynchronous triggering procedure begins when a 64 channel, FEE ASIC records a channel over threshold. A 64-fold *OR* is generated and passed to the next chip to the right or left. Eventually, this signal reaches a controller chip which then clears and starts a time-over-threshold (TOT) counter and a trigger-latency counter. A signal is sent to a tower controller which generates and distributes a trigger-acknowledge signal to the controller ASIC's in its and nearest neighbor towers. The value of the TOT counter is loaded into a FIFO buffer, and the trigger-acknowledge is passed to the FEE ASIC's which then load the outputs of the comparators into another FIFO buffer. The FIFO book-keeping is handled by the tower controller. Once a read command is sent to the controller ASIC's, the FIFO's of the FEE ASIC's are moved to a shift register and clocked out and the controller generates a token identifying the event. Once the read out of a plane is complete, the token and formatted data are passed to the next plane, and the process continues until all the planes of the tower have been read out and recorded by the tower controller. The architecture uses two separate event buffers to minimize effects of dead time.

3 Summary

With the goal of NASA mission approval in 2001 and a launch in 2004 into low Earth orbit, the GLAST collaboration has been developing a next generation, high energy gamma ray telescope. The GLAST research effort is now moving from developing individual components to optimizing these elements and developing and testing more integrated systems. In the fall of 1997, prototype silicon microstrip detectors and FEE ASIC's will be tested in a test beam at SLAC along with anticoincidence components and a CsI calorimeter. This will

be followed by the fabrication of a full-scale tower prototype. This will allow for end-to-end testing of all the components in the anticipated configuration in a test beam along with thermal, vibrational, and acoustical testing. In addition, a high altitude balloon flight of a full-scale tower is also being planned. Thus, the instrument will be tested in a flight configuration and under flight conditions.

References

[1] GLAST World Wide Web Page: *http://www-glast.stanford.edu*
GLAST Collaboration Institutions: NASA Ames Research Center; Boston University; University of Chicago; Columbia University; NASA Goddard Space Flight Center; ICTP and INFN, Trieste; Kanagawa University; Lockheed Martin Corporation, Palo Alto Research Center; Max Planck Institut fr Extraterrestrische Physik; U. S. Naval Research Laboratory; Ècole Polytechnique, IN2P3; University of Rome , INFN Roma2; CEA, Saclay; University of California, Santa Cruz; Shibaura Institute of Technology; Sonoma State University; Stanford Linear Accelerator Center; Stanford University; Texas A&M University-Kingsville; University of Tokyo; University of Utah; University of Washington

[2] For a review see C.E. Fichtel and D.J. Thompson, *High Energy Gamma Ray Astrophysics,* in *High Energy Astrophysics*, J.M. Matthews (editor), World Scientific (1994)

[3] D.J. Thompson, private communication

[4] C.E. Fichtel et al., A&A Suppl. Ser 97, 13 (1993)

[5] D.J. Thompson et al., APJS, 101 (1995)

[6] T.C. Weekes et al., *TeV Gamma Rays from Active Galactic Nuclei,* Proceedings of International Symposium on Extremely High Energy Cosmic Rays: Astrophysics and Future Observatories, Tanashi, Toyko, Japan (1996)

[7] D. Bertsch et al., ApJ, 405, L21 (1993)

[8] See for example, M.H. Salamon and F.W. Stecker, *Absorption of High Energy Gamma Rays by Interactions with Extragalactic Starlight Photons at High Redshifts*, 4th Compton Symposium (in press)

[9] See for example, M. Kamionkowski, *Diffuse Gamma Rays from WIMP Decay and Annihilation,* NATO Advanced Study Institute: The Gamma-Ray Sky with Compton GRO and Sigma (1994)

[10] J.T. Bonnell et al., *Gamma-ray Burst Studies with GLAST,* 25th ICRC, Vol. 3, 69 (1997)

[11] J.P. Norris et al., *Hodoscopic CsI Calorimeter for GLAST,*, 25th ICRC, Vol. 5, 77 (1997)

[12] W.B. Atwood, *GLAST: Applying silicon strip detector technology to the detection of gamma rays in space,* NIM A342, 302 (1994) and references therein.

[13] R. Brun et al., *GEANT: Simulation Program for Particle Physics Experiments,* CERN-DD/78/2, 1978

[14] A. Moiseev, NASA GSFC, private communication

[15] K. Michaud, *GLAST Trigger Requirements*, (1997), and J.E. Grove, *Particle Background Estimates for GLAST*, (1997), internal GLAST documents

[16] A. Luebke, Ph.D. Thesis, Stanford University (1996)

[17] *GLAST Thermal Modeling Results: Report to the Collaboration*, internal GLAST document (1997)

[18] W.B. Atwood, SLAC, *Design Issues for the GLAST Silicon Strip Pair-Conversion Telescope,* internal GLAST Document, (1997)

[19] I.A. Yadigaroglu, *Sensitivity of γ-ray Detectors to Polarization*, E-print, ASTROPH-9612129 (1996)

[20] C. Bedonie et al., *Capacitance of the GLAST Prototype Detectors,* internal GLAST Document, (1996)

[21] K. Ing et al., *Charge Collection in Silicon Strip Detectors with a Large Strip Pitch,* UCSC SCIPP Preprint 94/31, (1994)

[22] R.P. Johnson, private communication

[23] R.P. Johnson, *Conceptual Design of Front-End Readout Electronics for the GLAST Silicon-Strip Tracker*, internal GLAST document (1997)

Characteristics of GLAST Mission

primary instrument:	imaging pair conversion telescope
energy range:	~10 MeV to > 100 GeV
energy resolution:	~10%
effective area:	> 8000 cm^2 (> 1 GeV)
single photon angular resolution[1]:	< 3.3° x (100 MeV/E) (10 MeV to 3 GeV)
	< 0.12° (> 10 GeV)
field of view[2]:	> 2.5 steradians
point source sensitivity[3]:	1 day: 3×10^{-7} photons $cm^{-2}s^{-1}$
	1 year: 5×10^{-9} photons $cm^{-2}s^{-1}$
	5 years: 2×10^{-9} photons $cm^{-2}s^{-1}$
source location determination:	30 arcseconds to 5 arcminutes
mass:	3000 kg
power:	600 W
telemetry:	100 kbps
mission life:	> 2 years (planning for 5 years)
orbit:	low inclination
spacecraft pointing:	10 arcsecond knowledge; ~2° accuracy
operating modes:	all-sky survey mode, and pointed mode (any direction at any time)

1. 68% containment angle
2. full width at half
3. all-sky average, assumes scan-mode operation and high Galactic latitude

Table 1: The performance goals of the GLAST instrument.

16 Channel Performance (32 pF Input Load)			
Power (μW/channel)	Z_{In} (kΩ)	Shaping Time (μs)	ENC (electrons)
149	5.8	1.6	1170
115	6.5	2.0	1150
93	10.5	2.2	1550

Table 2: The performance of the 16 channel GLAST prototype, FEE ASIC.

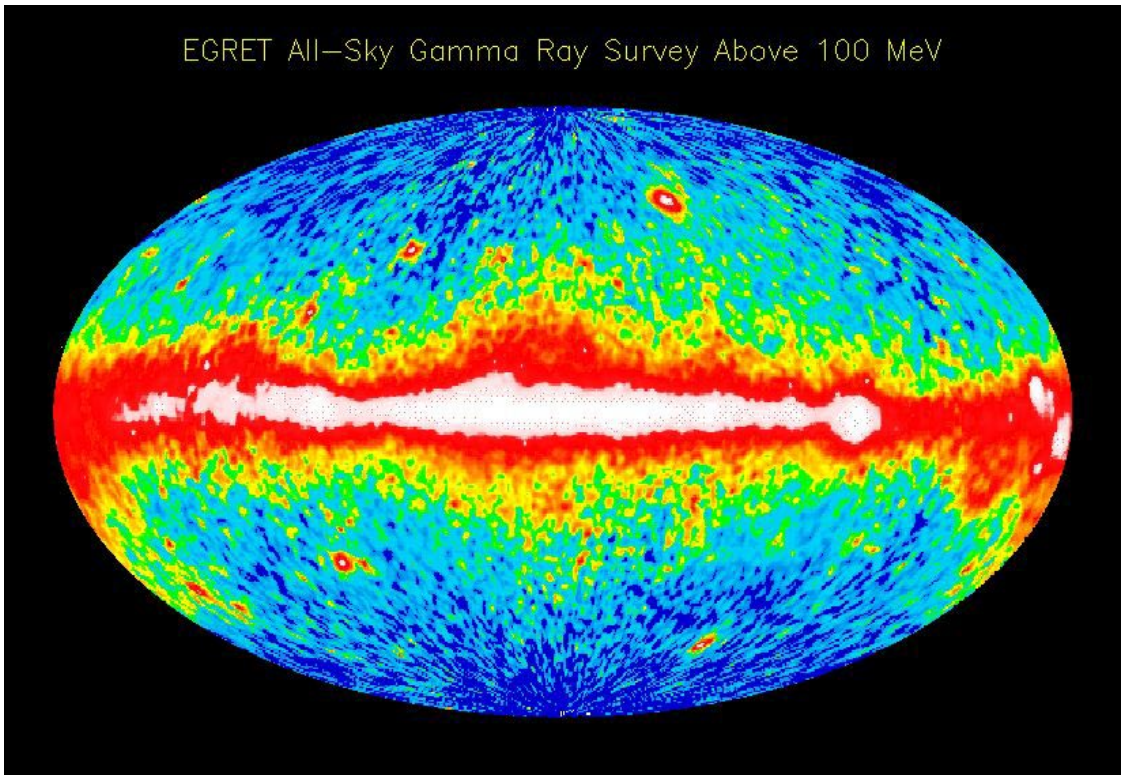

Fig. 1. The appearance of the universe as viewed by high energy gamma rays as a function of galactic coordinates (Courtesy of NASA).

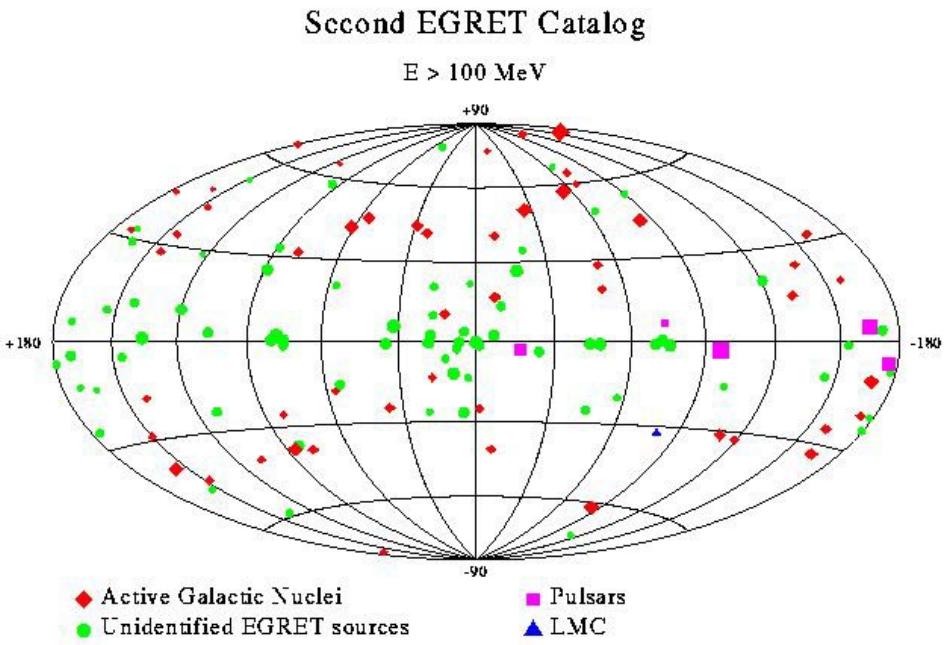

Fig. 2. The observed point sources of gamma rays with energy greater than 100 MeV from the Second Egret Catalog (D.J. Thompson et al., 1995).

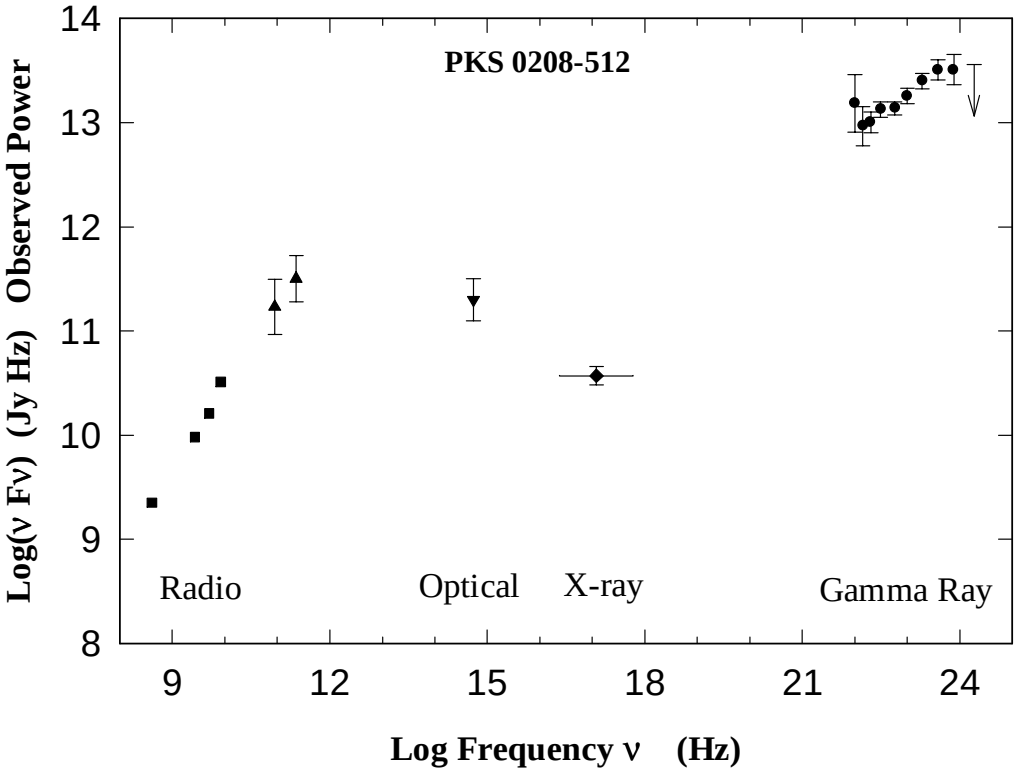

Fig. 3. The observed power spectrum from an AGN as a function of photon frequency (D. Bertsch et al., 1993).

Fig. 4. The conceptual design of the GLAST instrument.

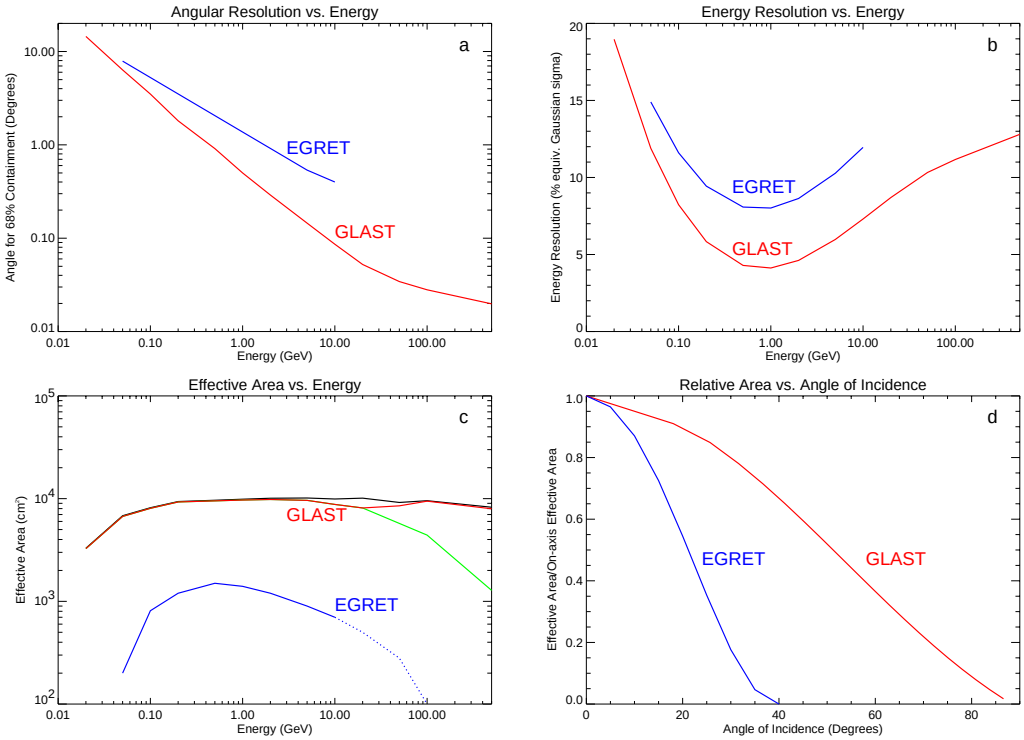

Fig. 5. Results from Monte Carlo studies illustrating the GLAST capabilities using EGRET as a metric for the parameters angular resolution (a), energy resolution (b), and effective area (c), as a function of incident photon energy and the relative area versus angular incidence (d) of the photon. In plot c, the black, upper curve is the effective area plot if the instrument is triggered on a gamma ray interaction in the tracker only, the red, middle curve is that for a trigger requiring a tracker gamma signature and either no veto in the anti-coincidence detector or greater then 5 GeV of energy deposited in the calorimeter. The green, lower curve represents a tracker gamma trigger and no anti-coincidence detector veto.

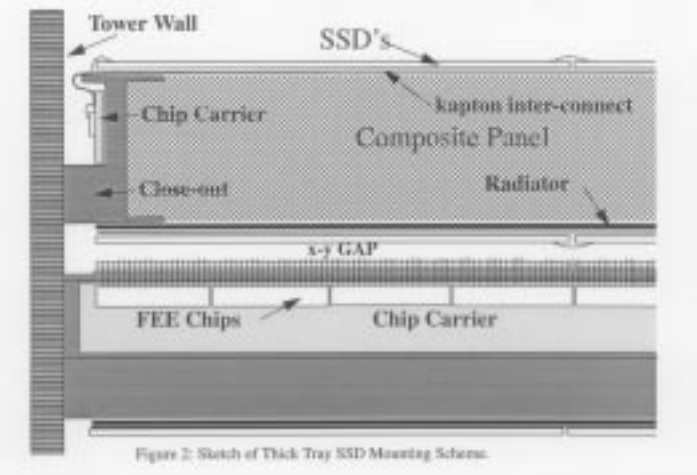

Fig. 6. A schematic view of a GLAST tower.

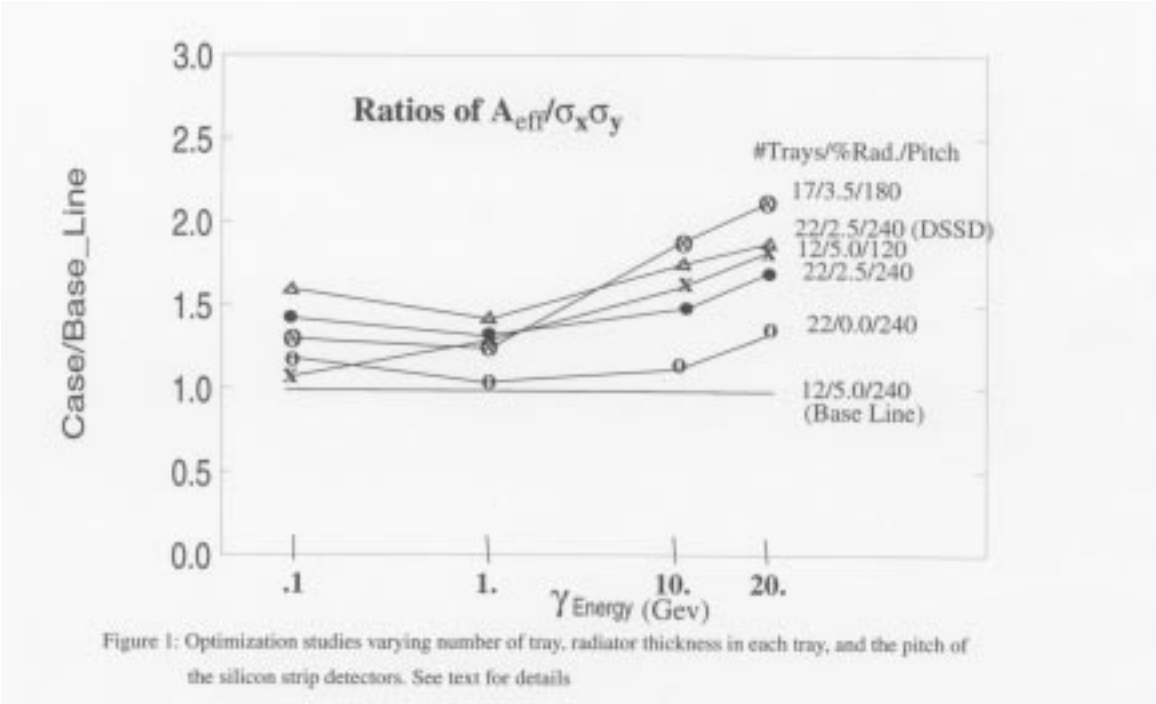

Figure 1: Optimization studies varying number of tray, radiator thickness in each tray, and the pitch of the silicon strip detectors. See text for details

Fig. 7. The results of the GLAST optimization Monte Carlo studies comparing the angular resolution of a variety of tracker designs to that of the initial baseline (Atwood, 1997).

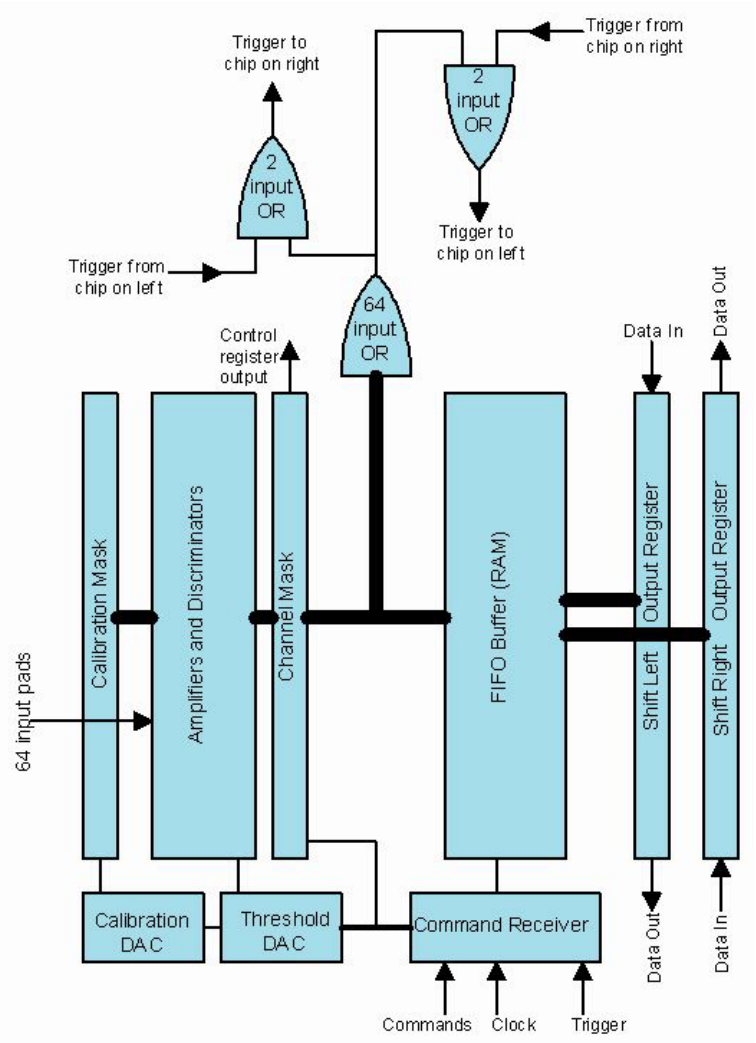

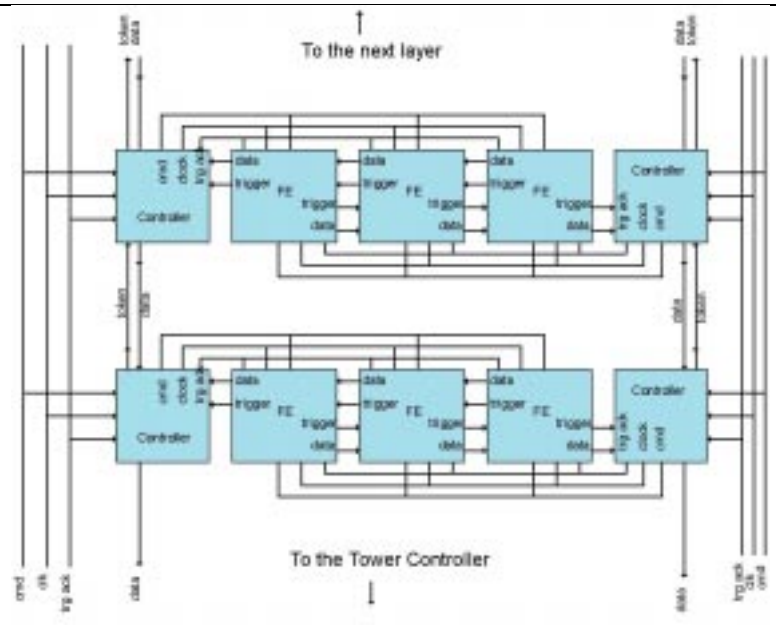

11.cm

Fig. 8. A schematic of the FEE ASIC architecture (top) and its implementation (bottom) in a GLAST tracker plane.